DEVELOPMENT OF A BEAM SWEEPING SYSTEM FOR THE FERMILAB ANTIPROTON SOURCE TARGET

F. M. Bieniosek, Fermilab, Batavia, IL 60510 USA*
O. Kurnaev, A. Cherepakhin, IHEP, Protvino, Russia
John Dinkel, Creative Designs, Inc.

Abstract

Intensity of the incident 120-GeV proton beam on the antiproton production target is scheduled to increase to $5x10^{12}$ protons per pulse. To prevent damage to the target, we plan to spread the hot spot on target with a beam sweeping system. Now under development are rotating-field magnets for installation upstream and downstream of the target. These magnets will deflect the beam in a circular pattern on the target. Peak current of 7 kA and peak voltage drop of 6 kV are expected. The power supply, which is separated from the magnet by a distance of about 10 m, utilizes magnetic pulse compression by saturating inductors to drive the magnets through the long transmission lines.

1 INTRODUCTION

Antiprotons are collected from the interaction of a 120-GeV proton beam with a solid nickel target. The efficiency of collecting antiprotons from the target rises as the size of the proton beam spot on the target is reduced. However at the same time the peak energy deposition on target rises. Estimates of the peak instantaneous energy deposition for the highest intensity achieved to date ($3.4x10^{12}$ protons per pulse) indicate an energy deposition of about 800 J/g. This is above the melting point of copper (about 600 J/g), and close to the melting point of nickel (about 1000 J/g). Under Main Injector conditions (5×10^{12} protons in a 1.6-μs pulse), the spot size will have to be increased to at least 0.25 mm to keep peak energy deposition near current levels. To bring the density of energy deposition with a 0.1-mm spot size down to currently-existing levels, a system to sweep the beam spot on the target will be required[1]. Several upgrades have been proposed for the Main Injector as part of the Tev33 project[2]. These upgrades (*e.g.* slip stacking) will result in increases in proton intensity of factors of 2-4 or more above the initial intensity of 5×10^{12}. Under these conditions sweeping becomes increasingly important, and larger sweep radii are required to restore the antiproton yield to its level at low intensity. The relative yield increase due to the sweeping system is about 15% for a 0.33-mm sweep radius at an intensity of 5×10^{12}, and 50% for a 0.5-mm sweep radius at a proton intensity of 1×10^{13}.

The upstream sweep magnets will be installed at the end of the AP1 beamline. The AP1 beamline transports and focuses the 120-GeV protons from the Main Ring onto the target. A pair of upstream magnets, placed at the downstream end of the AP1 beamline where the toroid M:TOR109 now resides, will sweep the 120-GeV proton beam. This location is near the focal point of the proton lithium lens, which may be used to focus 120-GeV proton beam on target. Antiprotons created in the target are collected by a lithium lens, and deflected by the pulsed magnet into the AP2 beam line for injection into the Debuncher. A single downstream sweep magnet placed in a double module between the collection lens and the pulsed magnet, near the focal point of the collection lens, will redirect the 8 GeV antiprotons exiting the collection lens parallel to the AP2 beamline. The portion of the antiproton flux that is focused by the lithium lens and collected downstream has a diameter of 22 mm. The magnet aperture radially inside the conductors is 28.5 mm.

2 SWEEP MAGNET

The beam sweeping system currently under development traces a 0.33-mm-radius circular pattern on the target over the 1.6-μs proton beam pulse. The magnets have a 2-phase, 4-conductor winding excited by two power supplies that deliver 625 kHz sinusoidal current waveforms in quadrature to generate a rotating dipole field[3]. The magnetic field due to two pairs of current-carrying conductors oriented 90° apart is rotating on axis if the current in the two pairs of conductors is $I_0 cos(\omega t)$ and $I_0 sin(\omega t)$. Figure 1 shows the magnetic field lines as calculated by POISSON at four times in the cycle. Currents to the horizontal and vertical pairs of conductors have a cos(ωt) and sin(ωt) time dependence, respectively.

The local field is itself not sufficiently uniform for use as a sweep magnet. However if the conductors are twisted such that the axial current distribution integrated over the length of the magnet has the distribution $sin\theta$ or $cos\theta$, respectively, the line integral of the field along the beam path is uniform and rotating. A design for the windings is indicated in Figure 2. The windings are in the form of two single-turn circuits placed symmetrically at 90-degree intervals. Each circuit has a twist of 180 degrees over the length of the magnet, such that $z=z_0 sin\theta$, where z_0 is an axial length, for example, half the length of the magnet. If $z_0/r_0 >> 1$ (long, thin magnet), the integrated axial current is distributed as $cos\theta$. The external power-supply connections for the two circuits are indicated respectively by the black and shaded circles. The end rings are

0-7803-4376-X/98/$10.00

common to the two circuits, and, if the magnet is driven by a bipolar power supply, are at ground potential. This magnet design is simple and mechanically robust. There are no breaks in the windings for power supply leads, and since the voltage is nominally zero at the ends, there is no need to allocate space to provide electrical insulation from neighboring devices in the target station.

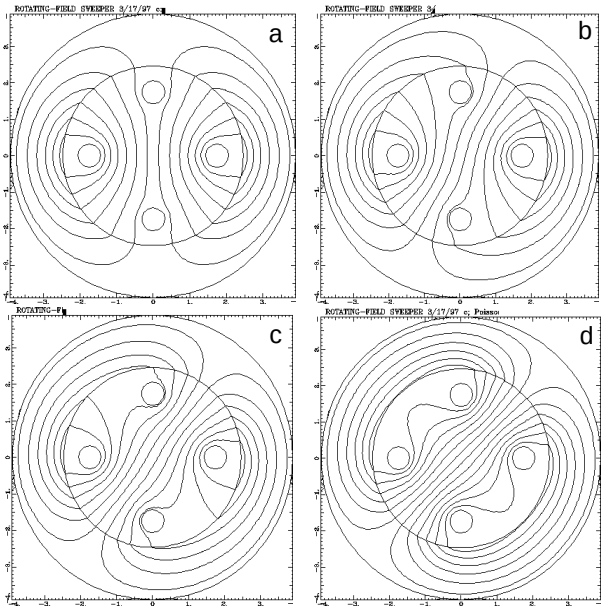

Figure 1. Local magnetic field structure for a 2-phase rotating-field sweep magnet. Field distribution is shown for (a) $\omega t=0$, (b) $\omega t=\pi/12$, (c) $\omega t=\pi/6$, (d) $\omega t=\pi/4$. A magnetic core surrounds the conductors. Dimensions are in cm.

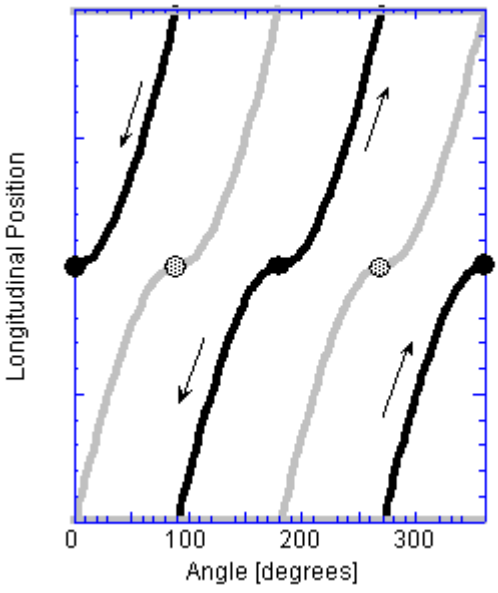

Figure 2. Shape of windings. The black curves represent one circuit, the gray curves represent the orthogonal circuit. Direction of current flow is indicated in one of the circuits.

Three identical magnets will be used, two upstream of the target, and one downstream. The sweeping radius is much smaller than the 2 cm diameter of the lithium collection lens and the aperture of the AP2 beam line. Each magnet is 56 cm long. The deflecting field is 900 G. An air gap is used since the beam is already transported through air from upstream of the target to downstream of the pulsed magnet.

MARS10 and CASIM calculations of energy deposition by hadron and electromagnetic cascades, supported by measurements on the high-voltage test module, show significant heating of iron and ferrite magnet cores downstream of the target. Total heating increases linearly with particle flux, and is a strong function of the radius of the magnet core. Three options for the composition of the magnetic core have been considered in detail.

1. Ferrite. Steady-state temperature rise of the core is determined by thermal conductivity of the material and the rate at which heat is removed at the surface. Because of the poor thermal conductivity and low Curie temperature ($T_c \cong 200°C$), it would be necessary to operate with a large inner-radius (3 cm) core and carefully cool the ferrite. Ferrite would need to be contained in case of cracking due to thermal stress.
2. Iron laminations. A laminated iron core does not have the thermal restrictions of a ferrite core. However very thin (<0.1 mm) laminations are required. Difficulties are expected in preparing and stacking the laminations.
3. Powder cores. The material chosen for the cores on the prototype magnet is 2-81 Mo-Permalloy pressed-powder (MPP). Construction with these cores is simple, and their relatively high thermal conductivity and Curie temperature ($T_c \cong 460°C$) significantly simplify the thermal restrictions compared to ferrites. The thermal stresses are small and can be contained by press-fitting the cores in a nickel housing. Eddy-current losses in the MPP material increase in intense radiation environments[4]. This is not likely to be a major concern, however, since the core is not the dominant loss mechanism in the circuit. A ceramic pipe will provide electrical insulation between the electrical conductors and the cores.

3 POWER SUPPLY

The sweep magnets must be provided with approximately 7 kA at 625-kHz by a power supply located on the floor of the AP0 service building. The current will be supplied through cables over a distance of approximately 10 m into the target vault, and by 2.5 m of strip line through steel shield modules to the magnets at the bottom of the target vault. The power supply circuit diagram is depicted in Figure 3a. Capacitor C3 is connected to the sweep magnet (inductance L3) via the strip line. Pulse compression is used to excite the ringing circuit L3, C3. Two-stage compression with saturated reactors has been chosen, which facilitates transfer of the current pulse to the ringing

circuit, and provides the capability to utilize a SCR switch for resonance charging of first stage capacitor C1 using a 1:10 step-up transformer. The reactors LS1 and LS2 are each composed of three 3.3-mV-sec/turn Metglas cores, wound with 10-μm Kapton insulation. The reactor LS1 has 16 turns and LS2 has 4 turns. The SPICE analysis (Figure 3b) shows that 5 kA peak current, 0.5 μs width is required to oscillate the magnet ringing circuit at 625 kHz with nominal 7 kA amplitude. The peak voltage amplitude at the magnet is 6 kV (3 kV to ground), with 8 kV (4 kV to ground) amplitude at ringing circuit capacitor C3. To achieve this, the first compression stage capacitor C1 should be charged to 17 kV. Taking into account the step-up transformer, the storage capacitor C0 charging voltage is 1.7 kV, the SCR switch peak current is 2 kA and the pulse duration is 15 μs. The power supply is designed to be capable of delivering 80% more current than nominal, for a 30 kV charge, to allow for possible future increase in beam sweeping radius. The magnet current pulse should be synchronized with the extracted beam with an accuracy of less than ±30 ns. Total delay in the power supply circuit, mainly due to the saturated reactors, is 25 μs at nominal current. This delay leads to a requirement on charging voltage stability of 10^{-3}, which is relatively easy to achieve. No other significant source of delay jitter has been observed, when testing a model power supply. The delay in the charging pulse also allows time to disable the Main Injector proton extraction kicker, in case of failure of the sweeping system charging supply.

4 HIGH-VOLTAGE TEST

Ionization of the air by the particle shower downstream of the target will increase the conductivity of the air between the conductors. Electrical losses through the ionized-air path across the gap reduce the Q of the circuit driving the magnet. A dummy test module was installed to measure the leakage current between two conductors symmetrically placed parallel to the beam path. Both the measurement and estimates based on CASIM calculations indicated a current drain between the plates on the order of 100 A, an acceptable amount. The measured leakage current is shown in Figure 4. The current through the air gap turned on rapidly at the beginning of the beam pulse and the gap rapidly opened after the end of the beam pulse. Avalanche ionization of the air is not a problem, as long as peak electric fields are kept well below breakdown levels, i.e. E<10 kV/cm. The test module was instrumented to provide information on heat dissipated and short-term magnetic effects in ferrite and tape-wound magnetic cores caused by the particle shower downstream of the target.

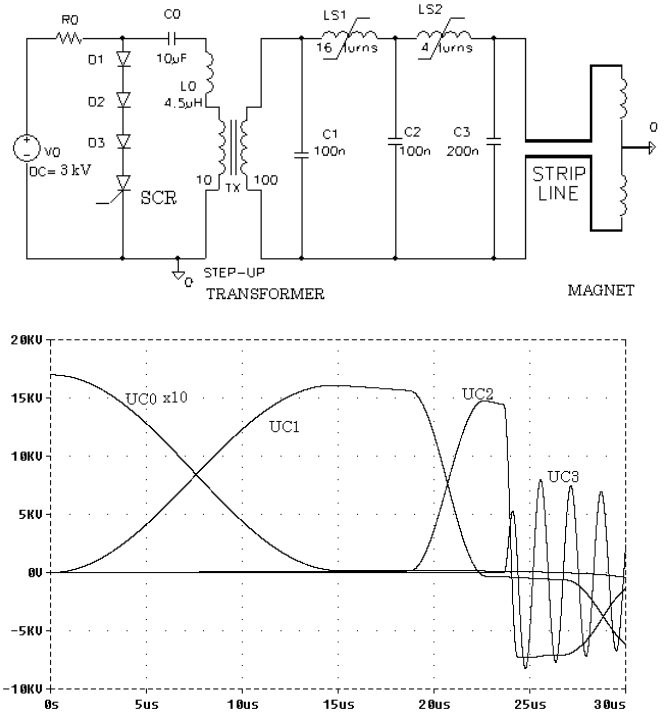

Figure 3. Sweep magnet power supply circuit. (a) SPICE circuit model, (b) voltage waveforms.

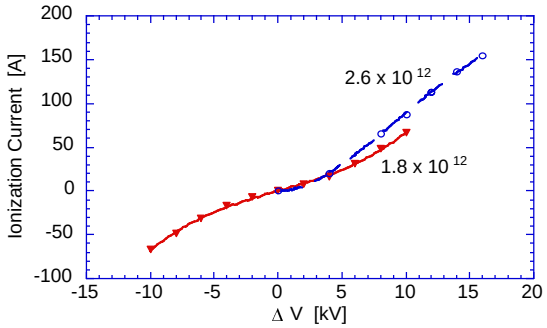

Figure 4. Measured leakage current during beam pulse between a pair of conductors 3-cm wide x 3-cm gap x 24-cm length as a function of voltage drop across the gap. Measurements were taken at two beam intensities.

---

*Operated by the Universities Research Association Inc., under contract with the U.S. Department of Energy.

[1] F. M. Bieniosek, A Beam Sweeping System for the Fermilab Antiproton Source, Fermilab-TM-1857 (1993). F. M. Bieniosek, K. Anderson, K. Fullett, Requirements for a Beam Sweeping System for the Fermilab Antiproton Source Target, Proc. 1995 US Particle Accelerator Conference.

[2] P. P. Bagley, et.al. Summary of the TeV33 Working Group, Proc. 1996 Snowmass Conf.

[3] F. M. Bieniosek, Beam-Sweep Magnet with Rotating Dipole Field, Pbar Note#561 (1996).

[4] C. W. Chen, Magnetism and Metallurgy of Soft Magnetic Materials, Dover, 1977, p. 474.